

## Supporting Information

**Reconsidering the *czcD* (NiCo) riboswitch as an iron riboswitch****Jiansong Xu and Joseph A. Cotruvo, Jr.\***

Department of Chemistry and Center for RNA Molecular Biology, The Pennsylvania State University, University Park, PA 16802 USA

\* Corresponding author. E-mail: juc96@psu.edu (J.A.C.).

This file contains Supplementary Tables S1-S5, Supplementary Figures S1-S7, and Supplementary References.

**SUPPLEMENTARY TABLES****Table S1.** Sequences of the DNA templates used for ITC and sensor studies**Table S2.** Primers used to generate or amplify DNA templates**Table S3.** Calculated  $K_{d,M}$  values used for determination of apparent  $K_{dS}$  of *czcD* sensors**Table S4.** Fluorescence response of **Lmo-2** to first-row transition metal ions**Table S5.** Fluorescence response of **Lmo-3** to first-row transition metal ions**SUPPLEMENTARY FIGURES****Figure S1.** Citrate-buffered fluorescence titrations of **Lmo-2** and **Lmo-3****Figure S2.** Representative thermograms from ITC studies of *Eba* with Ni<sup>II</sup>, Zn<sup>II</sup>, and Mn<sup>II</sup>**Figure S3.** Representative thermogram from ITC studies of the M3 variant of the *Eba* riboswitch**Figure S4.** Simulated ITC thermograms to estimate  $K_d$  for Mn<sup>II</sup> binding to *Eba***Figure S5.** Representative thermograms from ITC studies of *Eba* CG and UA variants with Co<sup>II</sup>**Figure S6.** Citrate-buffered fluorescence titrations of Co<sup>II</sup> and Fe<sup>II</sup> into Sensei sensors**Figure S7.** Representative thermograms from ITC studies of *Lmo* with Ni<sup>II</sup>, Zn<sup>II</sup>, and Mn<sup>II</sup>**SUPPLEMENTARY REFERENCES**

## SUPPLEMENTARY TABLES

**Table S1.** Sequences of the DNA templates used for the riboswitch ITC studies and riboswitch-based sensors. The DNA template sequences for the *Eba*, *Lmo*, and *Cce czd* riboswitches are derived from Furukawa et al.<sup>1</sup> Spinach2 sequences are shown in red.<sup>2</sup> In the sensor constructs, components of the appropriate truncated stem are shown in blue. Mutations present in the *Eba* variants are highlighted. Px-y denotes insertion of Spinach2 into stem x retaining y base pairs. Sensors **Lmo-1**, **Lmo-2**, and **Lmo-3** are the P1-1, P1-2, and P1-3 constructs.

Name	Sequence
<i>Eba</i>	5'- ccaagTAATACGACTCACTATAgAACTGAGCAGGCAAATGACCAGAGCGGTCATGCAGCCGGGCTG CGAAAGCGGCAACAGATGATTACACGCACATCTGTGGGACAGTT-3'
<i>Eba</i> -CG	5'- ccaagTAATACGACTCACTATAgAACTGAGCAcGCAAATGACCAGAGCGGTCATGCAGCcGGGGCTG CGAAAGCGGCAACAGATGATTACACGCACATCTGTGGGACAGTT-3'
<i>Eba</i> -UA	5'- ccaagTAATACGACTCACTATAgAACTGAGCAtGCAAATGACCAGAGCGGTCATGCAGCAAGGGGCTG CGAAAGCGGCAACAGATGATTACACGCACATCTGTGGGACAGTT-3'
<i>Lmo</i>	5'- ccaagTAATACGACTCACTATAgATCTGAACAGGCGGTGAACGTAACACGAGGTTTCATGCAGCTGG GCTGCAATTATTTGCGGCAGCAGACTATGTATTCTAAGGGCATATCTGTGGGACAGTT-3'
<i>Cce</i>	5'- ccaagTAATACGACTCACTATAgAACTGAGCAGGCGATGGACCTTTCATAGAGGTACATGGGGCCG GGCCACCCAGTGAGTGGCAGCAGATTGCAATCATGCACATCTGTGGGACAGTA-3'
Sensei	5'- ccaagTAATACGACTCACTATAGGTGGACGAAGTCGGCAGAGGTCCATTAGTCGGGGCCGTAGTC ACGGCAGCGGTTATTTTAGATCCACAACAGCCTATCCC-3'
Spinach2	5'- GATGTAAGTGAATGAAATGGTGAAGGACGGGTCCAGTAGGCTGCTTCGGCAGCCTACTTGTGTA GTAGAGTGTGAGCTCCGTAAGTACATC-3'
<i>Lmo</i> -1	5'- ccaagTAATACGACTCACTATAgGATGTAAGTGAATGAAATGGTGAAGGACGGGTCCAgaacaggcggtg aacgtaacacgaggttcatgcagctgggctgcaattatttgcggcagcagactatgtattctaagggcatatctgtgggaTTGTTGAGTA GAGTGTGAGCTCCGTAAGTACATC-3'
<i>Lmo</i> -2	5'- ccaagTAATACGACTCACTATAgGATGTAAGTGAATGAAATGGTGAAGGACGGGTCCAtgaacaggcggt gaacgtaacacgaggttcatgcagctgggctgcaattatttgcggcagcagactatgtattctaagggcatatctgtgggaTTGTTGAG TAGAGTGTGAGCTCCGTAAGTACATC-3'
<i>Lmo</i> -3	5'- ccaagTAATACGACTCACTATAgGATGTAAGTGAATGAAATGGTGAAGGACGGGTCCActgaacaggcgg tgaacgtaacacgaggttcatgcagctgggctgcaattatttgcggcagcagactatgtattctaagggcatatctgtgggacagTTGTTGA GTAGAGTGTGAGCTCCGTAAGTACATC-3'
Sensei P1-2	5'- ccaagTAATACGACTCACTATAgATGTAAGTGAATGAAATGGTGAAGGACGGGTCCAGGACGAAGT CGGCAGAGGTCCATTAGTCGGGGCCGTAGTCACGGCAGCGGTTATTTTAGATCCACAACAGCCT TTGTTGAGTAGAGTGTGAGCTCCGTAAGTACATC-3'
Sensei P1-3	5'- ccaagTAATACGACTCACTATAgATGTAAGTGAATGAAATGGTGAAGGACGGGTCCAtGGACGAAGT CGGCAGAGGTCCATTAGTCGGGGCCGTAGTCACGGCAGCGGTTATTTTAGATCCACAACAGCCT ATTGTTGAGTAGAGTGTGAGCTCCGTAAGTACATC-3'
Sensei P1-4	5'- ccaagTAATACGACTCACTATAgATGTAAGTGAATGAAATGGTGAAGGACGGGTCCAgTGGACGAAG TCGGCAGAGGTCCATTAGTCGGGGCCGTAGTCACGGCAGCGGTTATTTTAGATCCACAACAGCC TATTGTTGAGTAGAGTGTGAGCTCCGTAAGTACATC-3'

**Table S2.** Primers used to generate or amplify DNA templates

<b>Name</b>	<b>Sequence</b>
Eba-top	5'- CCAAGTAATACGACTCACTATAGAACTGAGCAGGCAAATGACCAGAGCGGTCATGCAGC CGGGCTGCGAAA-3'
Eba-bottom	5'- AACTGTCCCACAGATGTGCGTGTAAATCATCTGTTGCCGCTTTCGCAGCCCCGGCTGCATGA C-3'
Eba-CG-top	5'- ccaagTAATACGACTCACTATAgAACTGAGCAGCAAATGACCAGAGCGGTCATGCAGCGG GGCTGCGAAA-3'
Eba-CG-bottom	5'- AACTGTCCCACAGATGTGCGTGTAAATCATCTGTTGCCGCTTTCGCAGCCCCGGCTGCATGA C-3'
Eba-UA-top	5'- ccaagTAATACGACTCACTATAgAACTGAGCATGCAAATGACCAGAGCGGTCATGCAGCAG GGCTGCGAAA-3'
Eba-UA-bottom	5'- AACTGTCCCACAGATGTGCGTGTAAATCATCTGTTGCCGCTTTCGCAGCCCTGCTGCATGA C-3'
Lmo-top	5'- CCAAGTAATACGACTCACTATAGATCTGAACAGGCGGTGAACGTAACACGAGGTTTCATGC AGCTGGGCTGCAATT-3'
Lmo-bottom	5'- AACTGTCCCACAGATATGCCCTTAGAATACATAGTCTGCTGCCGCAAATAATTGCAGCCC AGCTGC-3'
Cce-top	5'- CCAAGTAATACGACTCACTATAGAACTGAGCAGGCGATGGACCTTTCATAGAGGTACATG GGCCGGGCCACCCAGTGAGT-3'
Cce-bottom	5'- TACTGTCCCACAGATGTGCATGATTGCAATCTGCTGCCACTCACTGGGTGGCCC -3'
Sensei-top	5'- CCAAGTAATACGACTCACTATAGGTGGACGAAGTCGGCAGAGGTCCATTAGTCGGGGCC GTAGTCA-3'
Sensei-bottom	5'- GGGATAGGCTGTTGTGGATCTAAAATAACCGCTGCCGTGACTACGGCCCCGACTAATGG A-3'
Lmo_P1-3_fwd	5'-GATGTAAGTGAATGAAATGGTGAAGGACGGGTCCACTGAACAGGCGGTGAACG-3'
Lmo_P1-3_rev	5'- GATGTAAGTGAATGAAATGGTGAAGGACGGGTCCACTGAACAGGCGGTGAACG-3'
Lmo_P1-2_fwd	5'-GATGTAAGTGAATGAAATGGTGAAGGACGGGTCCACTGAACAGGCGGTGAACG-3'
Lmo_P1-2_rev	5'- GATGTAAGTGAATGAAATGGTGAAGGACGGGTCCACTGAACAGGCGGTGAACG-3'
Lmo_P1-1_fwd	5'-GATGTAAGTGAATGAAATGGTGAAGGACGGGTCCACTGAACAGGCGGTGAACG-3'
Lmo_P1-1_rev	5'- GATGTAAGTGAATGAAATGGTGAAGGACGGGTCCACTGAACAGGCGGTGAACG-3'
T7_Sp2_Amp_fwd	5'-CCAAGTAATACGACTCACTATAGGATGTAAGT-3'
Sp2_Amp_rev	5'-GATGTAAGTGAATGAAATGGTGAAGGACGGGTCCACTGAACAGGCGGTGAACG-3'

**Table S3.** Calculated  $K_{d,M}$  values (effective  $K_d$  values for metal-citrate buffers) used for determination of apparent  $K_{d,s}$  of *czcD* sensors. For full details, see the Supporting Information of Xu and Cotruvo.<sup>3</sup>

Chelator	Metal	log $K_M$	Adjusted $K_{d,M}$
Citric acid	Mn <sup>II</sup>	4.15	$7.30 \times 10^{-5}$
	Fe <sup>II</sup>	4.40	$4.10 \times 10^{-5}$
	Co <sup>II</sup>	5.00	$1.05 \times 10^{-5}$
	Ni <sup>II</sup>	5.40	$4.10 \times 10^{-6}$
	Zn <sup>II</sup>	4.98	$1.08 \times 10^{-6}$
	Mg <sup>II</sup>	3.37	$4.60 \times 10^{-4}$

**Table S4.** Fluorescence response of **Lmo-2** to first-row transition metal ions (see **Figure S1A**)

	Mn <sup>II</sup>	Fe <sup>II</sup>	Co <sup>II</sup>	Ni <sup>II</sup>	Zn <sup>II</sup>
$K_{d,app}$ (nM)	$5900 \pm 200$	$270 \pm 10$	$64 \pm 2$	$52 \pm 3$	$1969 \pm 60$
$F_{max}/F_{min}$	3.9	4.1	5.1	4.0	4.6
Hill coefficient ( $n$ )	$2.1 \pm 0.1$	$2.9 \pm 0.4$	$1.9 \pm 0.1$	$1.5 \pm 0.1$	$2.2 \pm 0.1$

Conditions: 30 mM MOPS, 100 mM KCl, 3 mM MgCl<sub>2</sub>, 1 mM citrate pH 7.2, 20 °C; 100 nM **Lmo-3**, 10 μM DFHBI-1T

**Table S5.** Fluorescence response of **Lmo-3** to first-row transition metal ions (see **Figure S1B**)

	Mn <sup>II</sup>	Fe <sup>II</sup>	Co <sup>II</sup>	Ni <sup>II</sup>	Zn <sup>II</sup>
$K_{d,app}$ (nM)	N.R. <sup>a</sup>	$2700 \pm 200$	$820 \pm 100$	$290 \pm 30$	N.R.
$F_{max}/F_{min}$	N.D. <sup>b</sup>	12.8	15.2	13.6	N.D.
Hill coefficient ( $n$ )	N.D.	$2.5 \pm 0.2$	$2.8 \pm 0.5$	$2.2 \pm 0.3$	N.D.

<sup>a</sup> N.R.: No response detected. <sup>b</sup> N.D.: Not determined. Conditions: 30 mM MOPS, 100 mM KCl, 3 mM MgCl<sub>2</sub>, 1 mM citrate pH 7.2, 20 °C; 100 nM **Lmo-3**, 10 μM DFHBI-1T

## SUPPLEMENTARY FIGURES

**Figure S1.** Citrate-buffered fluorescence titrations of (A) **Lmo-2** and (B) **Lmo-3** with  $\text{Mn}^{\text{II}}$ ,  $\text{Fe}^{\text{II}}$ ,  $\text{Co}^{\text{II}}$ ,  $\text{Ni}^{\text{II}}$ , and  $\text{Zn}^{\text{II}}$ . For each construct, fluorescence response was evaluated by titrating metal into 100 nM sensor and 10  $\mu\text{M}$  DFHBI-1T, in 30 mM MOPS, 100 mM KCl, 3 mM  $\text{MgCl}_2$ , and 1 mM citrate, pH 7.2, at 20 °C. (C) Representation of the sensor constructs, illustrating the junction between the P1 stem and Spinach2, with **Lmo-1** and **Lmo-2** given as examples.

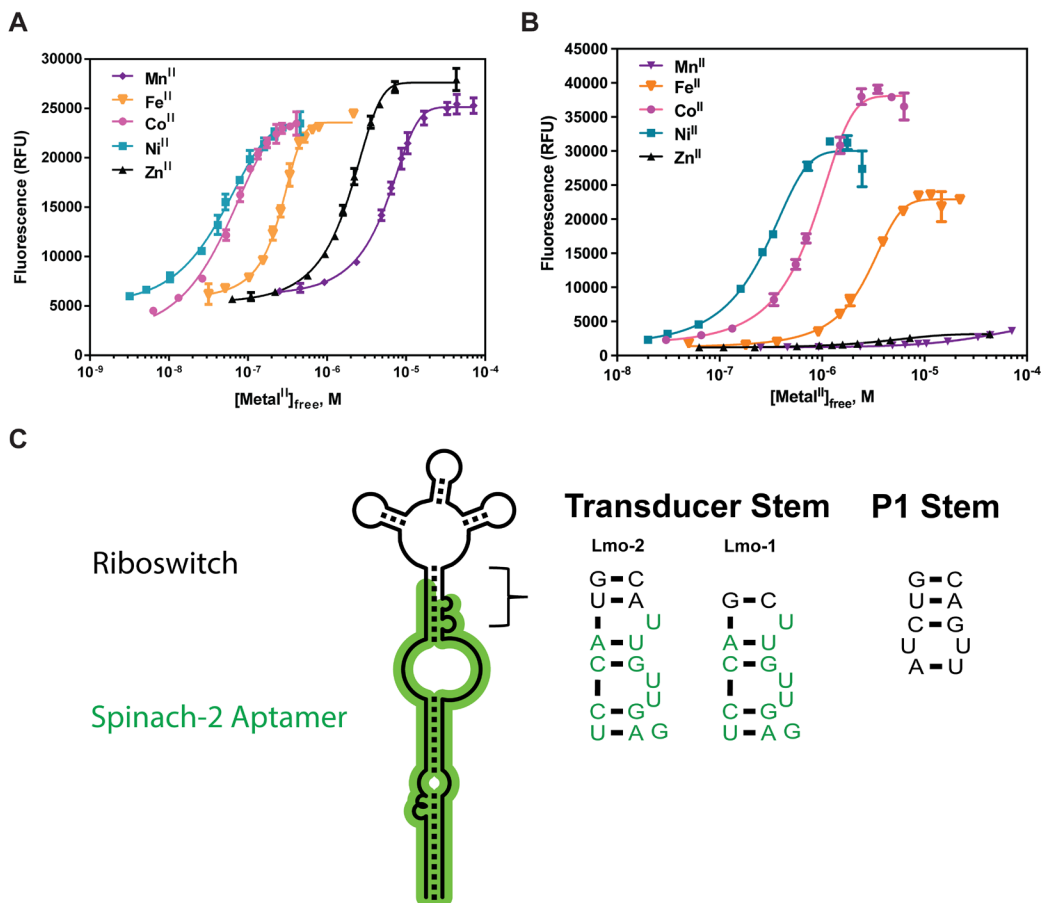


**Figure S2.** Representative thermograms from ITC studies of the *Eba* riboswitch (9.4-11  $\mu$ M RNA) with  $\text{Ni}^{\text{II}}$ ,  $\text{Zn}^{\text{II}}$ , and  $\text{Mn}^{\text{II}}$ . The data are fitted to a model with one set of equivalent binding sites. Experimental conditions and fitted parameters are provided in **Table 2**.

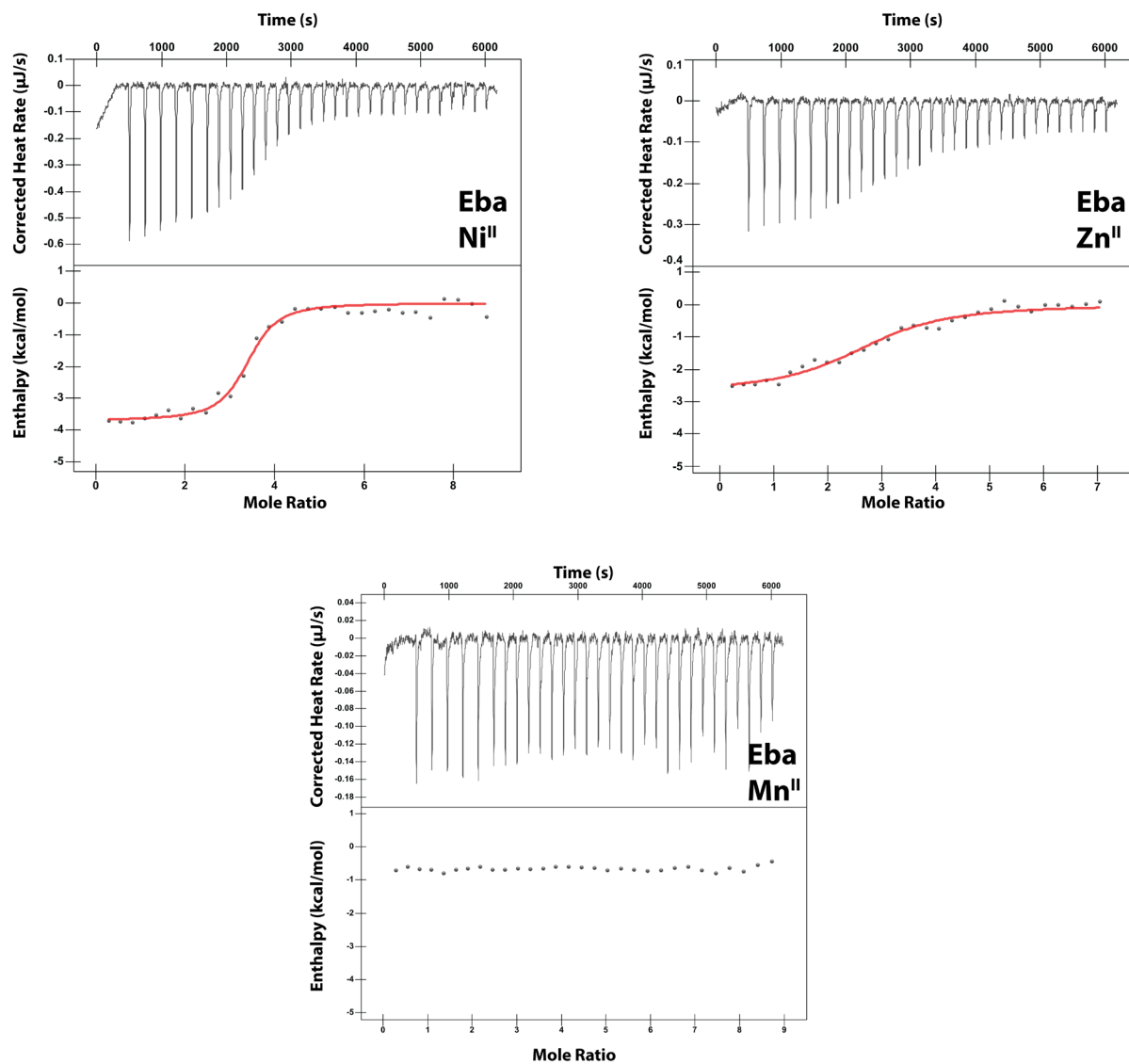


**Figure S3.** Representative thermogram from ITC studies of the M3 variant of the *Eba* riboswitch (8  $\mu\text{M}$  RNA) with  $\text{Co}^{\text{II}}$ . The data are fitted to a model with one set of equivalent binding sites. Conditions: 30 mM MOPS, 100 mM KCl, 3 mM  $\text{MgCl}_2$ , pH 7.2, 20  $^{\circ}\text{C}$ .

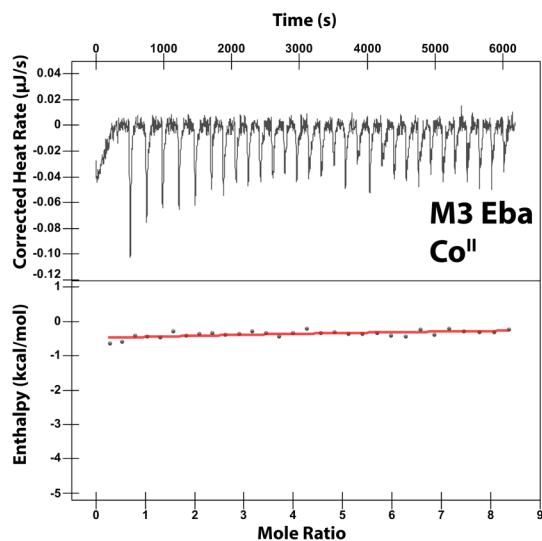


**Figure S4.** Simulated ITC thermograms for metal ion binding to the *Eba* riboswitch, to estimate  $K_{\text{d,app}}$  for  $\text{Mn}^{\text{II}}\text{-Eba}$ . Simulation parameters are based on the experimental parameters for other metal ions (10  $\mu\text{M}$  RNA in cell, 600  $\mu\text{M}$  metal ion in syringe,  $30 \times 1.2 \mu\text{L}$  injections, 20  $^{\circ}\text{C}$ ) and  $n = 3$  and  $\Delta H = -4.5 \text{ kcal/mol}$ . Comparing to the experimental data in **Figure S2**, we suggest a  $K_{\text{d,app}}$  between 0.1 and 1 mM.

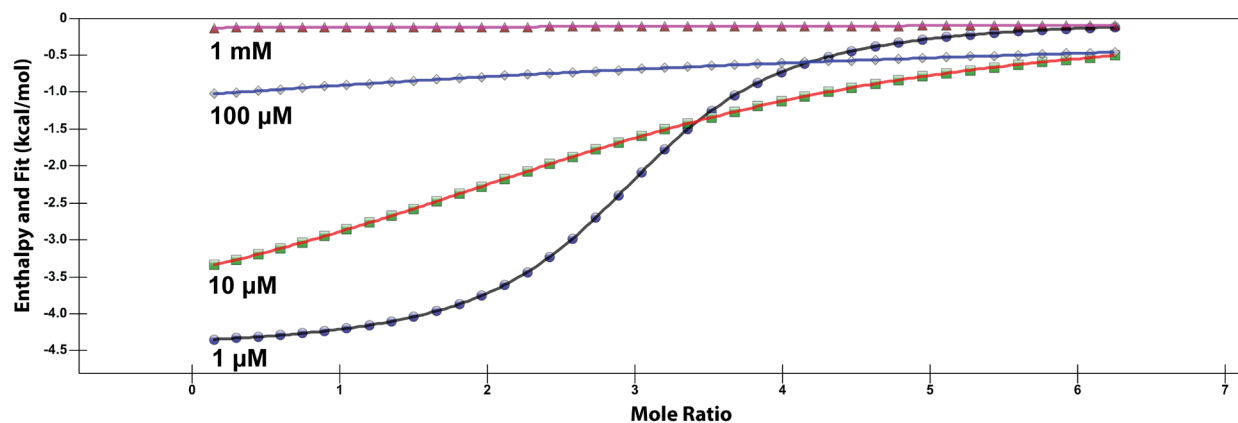


**Figure S5.** Representative thermograms from ITC studies of the CG and UA variants of the *Eba* riboswitch (8.5-11  $\mu\text{M}$ ) with  $\text{Co}^{\text{II}}$ . The data are fitted to a model with one set of equivalent binding sites. Experimental conditions and fitted parameters are provided in **Table 2**.

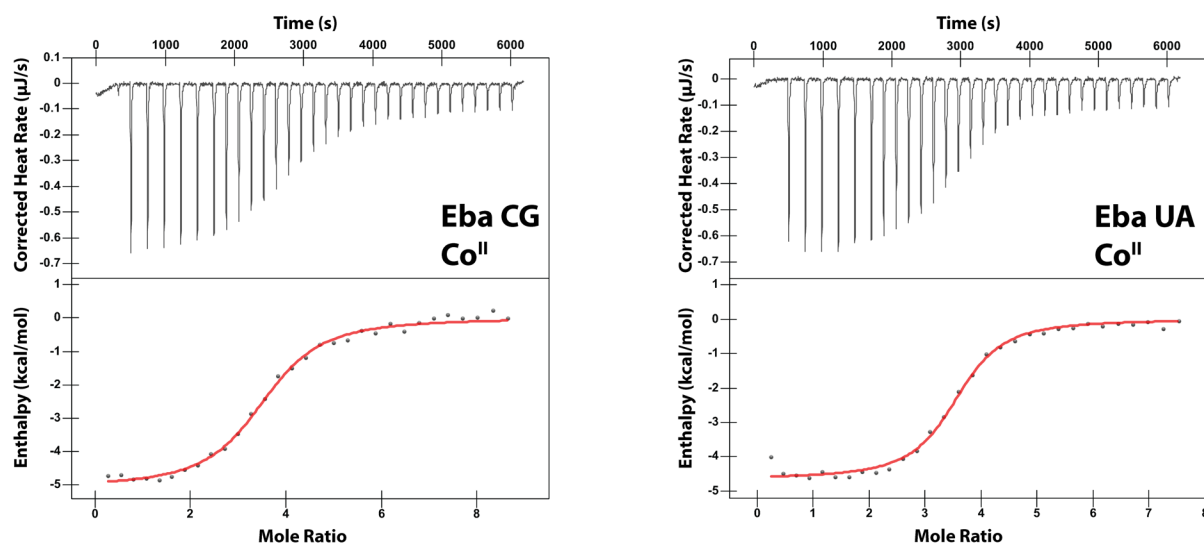


**Figure S6.** Citrate-buffered fluorescence titrations of (A)  $\text{Co}^{\text{II}}$  and (B)  $\text{Fe}^{\text{II}}$  into Sensei sensors. For each construct, fluorescence response was evaluated by titrating metal into 100 nM sensor and 10  $\mu\text{M}$  DFHBI-1T, in 30 mM MOPS, 100 mM KCl, 3 mM  $\text{MgCl}_2$ , and 1 mM citrate, pH 7.2, at 20  $^{\circ}\text{C}$ . The sensors did not show any fluorescence activation with the metals.

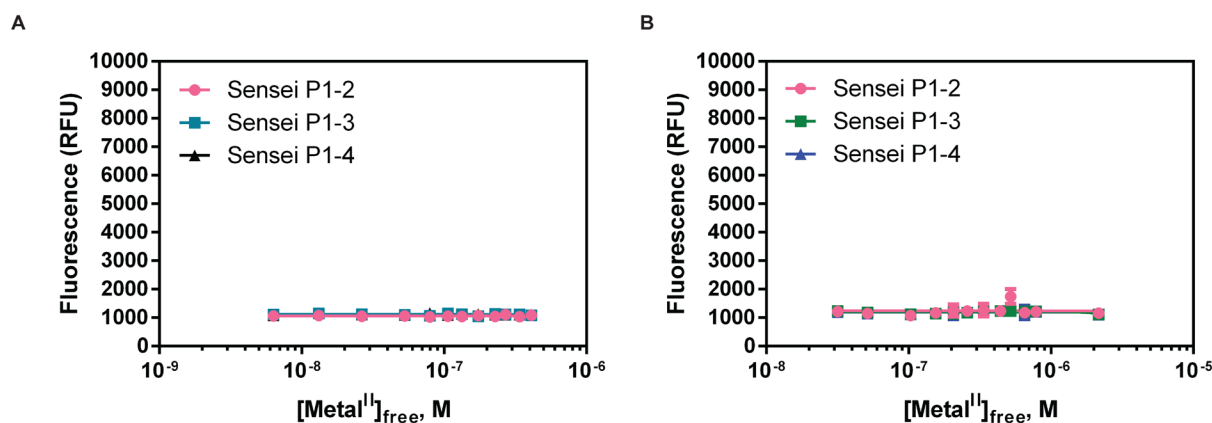
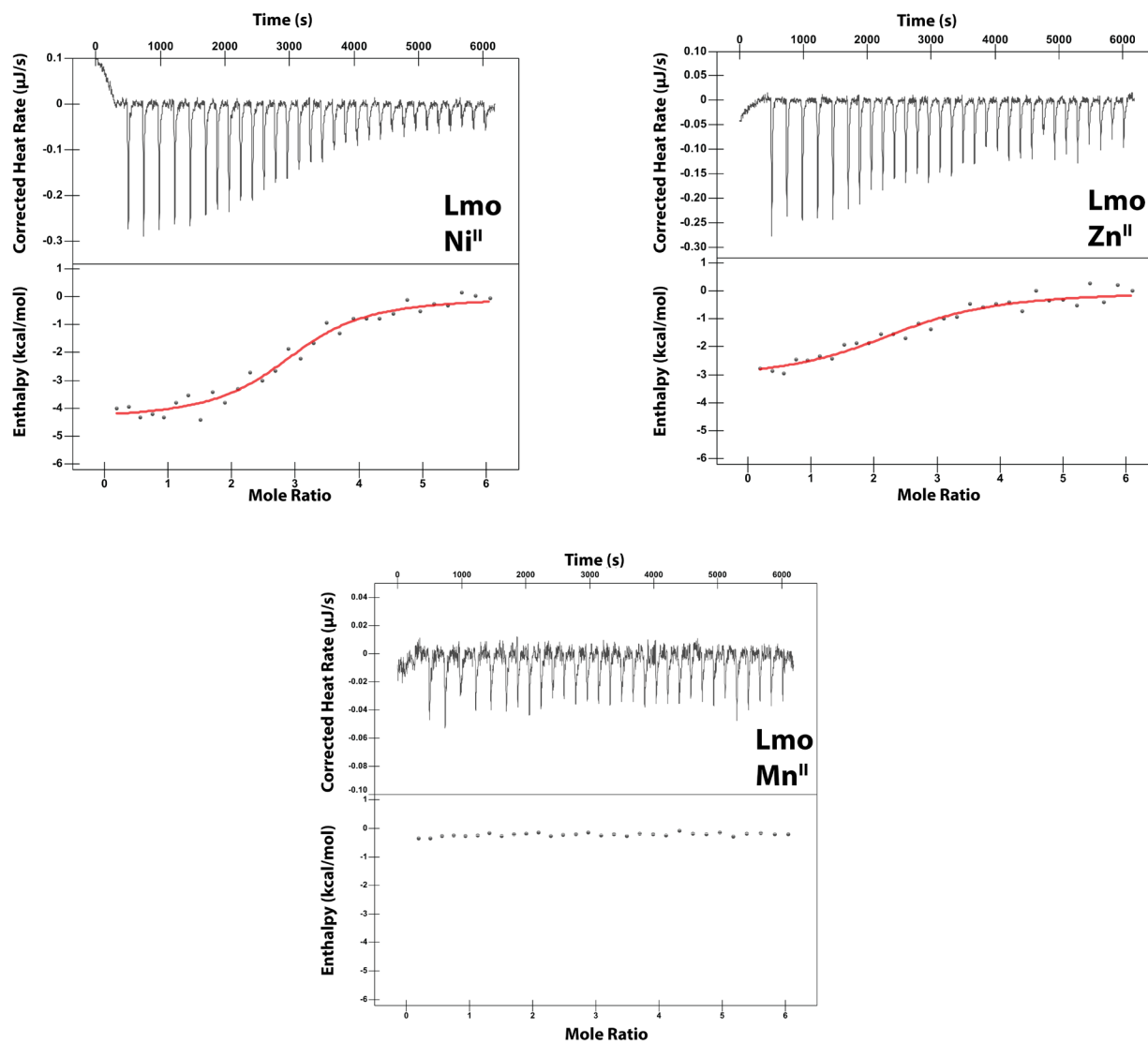




**Figure S7.** Representative thermograms from ITC studies of the *Lmo* riboswitch (8-10  $\mu$ M RNA) with  $\text{Ni}^{\text{II}}$ ,  $\text{Zn}^{\text{II}}$ , and  $\text{Mn}^{\text{II}}$ . The data are fitted to a model with one set of equivalent binding sites. Experimental conditions and fitted parameters are provided in **Table 2**.



**REFERENCES**

1. Furukawa, K.; Ramesh, A.; Zhou, Z.; Weinberg, Z.; Vallery, T.; Winkler, W. C.; Breaker, R. R., Bacterial riboswitches cooperatively bind Ni<sup>2+</sup> or Co<sup>2+</sup> ions and control expression of heavy metal transporters. *Mol. Cell* **2015**, *57*, 1088-1098.
2. Strack, R. L.; Disney, M. D.; Jaffrey, S. R., A superfolding Spinach2 reveals the dynamic nature of trinucleotide repeat-containing RNA. *Nat. Methods* **2013**, *10*, 1219-1224.
3. Xu, J.; Cotruvo, J. A. J., The *czcD* (NiCo) riboswitch responds to iron(II). *Biochemistry* **2020**, *59*, 1508-1516.